# Studies of Phospholipid Vesicle Deposition/Transformation on a Polymer Surface by Dissipative Quartz Crystal Microbalance and Atomic Force Microscopy

**Yecang Tang, Zhining Wang, Junwu Xiao, and Shihe Yang***

*Department of Chemistry, The Hong Kong University of Science and Technology, Clear Water Bay, Kowloon, Hong Kong, China*

**Yong Jian Wang and Penger Tong**

*Department of Physics, The Hong Kong University of Science and Technology, Clear Water Bay, Kowloon, Hong Kong, China*

*Received: July 19, 2009; Revised Manuscript Received: September 4, 2009*

Polymer-supported phospholipid bilayers (PLBs) are popular model systems for the study of transmembrane proteins under conditions close to cellular membrane environments. In this work, by combining the techniques of dissipative quartz crystal microbalance and atomic force microscopy, we investigate the deposition of vesicles on a hydrated cationic poly(diallyldimethylammonium chloride) (PDDA) layer as a function of phospholipid composition and sodium chloride concentration. The vesicles used consist of phospholipid mixtures with varying amounts of net negative charge. Uniform PLBs are formed by either increasing the negative charge density of the vesicles or decreasing sodium chloride concentration, suggesting that the electrostatic attraction between the vesicle and PDDA layer is the driving force for the formation of the PLBs. Our results indicate that the PLB formation is a fast adsorption−rupture process of the vesicles, without passing through a critical vesicle density. We further contend that the fluctuating PDDA support plays a central role for this process. This work provides a framework for understanding the key factors that influence the formation of PLBs.

## Introduction

Supported phospholipid bilayers have been used extensively as a well-defined model system to understand the structures and functions of biomembranes,[1−4] such as cell adhesion[5] and protein interactions,[6] and to design biosensors.[7] Many studies in the past decade focused on solid-supported phospholipid bilayers (SLBs). Phospholipid vesicles readily spread and self-assemble to form bilayers on hydrophilic solid substrates, such as glass, $SiO_2$, and mica surfaces. These bilayers show good fluidity due to a thin (1−2 nm) lubricating layer of water between the bilayer and substrate. However, the use of the SLBs is severely limited by the adverse effects of the solid substrate. Because of the close proximity of the bilayer to the solid surface, transmembrane proteins in an SLB inevitably interact with the underlying substrate. This interaction with the substrate can in turn cause proteins in the bilayer to become immobile, hinder their function, and even lead to their denaturation. To overcome this problem, it was suggested that a hydrophilic polymer layer is inserted between the substrate and the phospholipid bilayer, forming the so-called polymer-supported phospholipid bilayers (PLBs).[7] This polymer cushion separates the bilayer from the solid substrate, reducing the frictional coupling between proteins and the substrates, and maintains the mobility of the membrane constituents.[7] While it is difficult to directly form phospholipid bilayers on many solid substrates, such as metals, metal oxides, and semiconductor electrodes, the polymer films can help to couple the bilayers to these substrates for transducing electrical signals and designing biosensors.

Polyelectrolytes,[8−16] lipopolymers[17−26] and biomacromolecules such as chitosan,[27] cellulose,[28,29] and streptavidin[30] have been explored for supporting phospholipid bilayers. One strategy is to insert polymers with covalently attached phospholipid analogues doped in the lower leaflet of phospholipid bilayers, which secures the polymer−bilayer interface. In addition, lipopolymers can be tethered to the solid substrate via sulfur−metal bond formation,[17,18] silane bonding,[24−26] or photoreactive coupling,[19,20,31] By adjusting the thickness and density of the polymer layer, the bilayer−solid distance and the viscosity in between can be tuned, both of which control the lateral mobility and function of the phospholipid bilayer.[21]

Another feasible strategy is to use hydrated polyelectrolyte films as soft cushions for phospholipid bilayers. A single layer of polyethylenimine was used to support phospholipid bilayers.[12−14] Also designed were organic double layers consisting of a self-assembled monolayer (SAM) of 11-mercaptoundecanoic acid (MUA) on gold surface and above it a thin layer of hydrated cationic poly(diallyldimethylammonium chloride) (PDDA). Negatively charged phospholipid bilayers have been successfully constructed on such a PDDA/MUA layer pair.[8−10] Here, electrostatic, van der Waals, and hydrogen bonding interactions are thought to play important roles in binding the phospholipid layers to the polymer cushions. In the preparation of PLBs, the phospholipid composition and ionic strength and pH of the solution are also expected to influence the polymer chain conformation and the polymer−substrate and polymer−bilayer interactions, all of which will have an impact on the kinetics of bilayer formation and the physical properties of the final bilayer thus formed.[2] Despite all the efforts to date, uniform PLBs were seldom reported and/or confirmed by in situ imaging techniques

* To whom correspondence should be addressed. E-mail: chsyang@ust.hk.

10.1021/jp9068224 CCC: $40.75 
Published on Web 10/09/2009

such as atomic force microscopy (AFM), not mentioning systematic studies of vesicle deposition processes on soft polymer layers.

Dissipative quartz crystal microbalance (QCM-D)[32−34] and AFM[11,33,35,36] as powerful surface analytical tools have been used in situ to probe the vesicle adsorption/fusion and formation of phospholipid bilayers. The QCM-D provides two parameters simultaneously: the adsorbed mass (as a frequency shift) and the surface viscoelastic behavior (as a change in dissipation).[37] Particularly important is its ability to distinguish between adsorbed intact vesicles (high dissipation) and bilayers (low dissipation) by the dissipation parameter, and thereby to monitor the vesicle-to-bilayer transformation in real time.[38] Using the QCM-D technique, Kasemo et al.[34] studied the effect of temperature, size of vesicles, surface nature, and osmotic pressure on SLB formation. Richter et al.[39] used QCM-D to distinguish four different pathways of vesicle deposition on solid surfaces. On the other hand, AFM is a surface specific technique with high spatial resolution, which can provide topological information, such as the morphology of a single vesicle and isolated bilayer patches, particularly useful for the study of the assembled structures of phospholipids. Moreover, AFM has emerged as a unique tool to investigate defects in bilayers down to nanometer scale. The combination of the two techniques will not only help us to qualitatively understand the bilayer formation but also provide an opportunity for a more quantitative assessment of its dynamic process.[39]

In the work reported below, we use both techniques to investigate the deposition of phospholipid vesicles on a PDDA/MUA layer. We systematically study the effects of phospholipid composition and sodium chloride concentration on PLB formation, which provides new insights into the roles played by the soft polymer cushion and the electrostatic interaction in the process of PLB assembly. The results afford a fairly comprehensive picture about the phospholipid vesicle deposition, rearrangement, and assembly on the polymer film and lay the foundation for the further design, fabrication, and perfection of PLBs.

## Materials and Methods

**Materials.** 1,2-Dioleoyl-*sn*-glycero-3-phosphocholine (DOPC, purity >99%) and 1,2-dioleoyl-*sn*-glycero-3-phospho-*rac*-(1-glycerol) sodium salt (DOPG, purity >99%) were purchased from Avanti Polar Lipids (Alabaster, AL). MUA (95%) and PDDA ($M_w$ 400 000−500 000, 20% w/w water solution) were obtained from Sigma-Aldrich (St. Louis, MO). 1-Monooleoyl glycerol (MO, purity >95%) was purchased from Danisco Cultor (Denmark). Other reagents used including chloroform (99.8%, Laboratory-Scan Ltd.), tris(hydroxymethyl)aminomethane (Tris, 99.9+%, Aldrich), and sodium chloride (99.8%, Riedel-deHaën) were of the highest purity available. All the chemicals were used without further purification.

The buffer solutions used throughout the experiment were Tris buffer containing 10 mM Tris and 100 mM NaCl except in the study of the NaCl concentration effect. The pH was adjusted to 8.0 with a 2.0 M HCl solution. Milli-Q water (Barnstead, compact ultrapure water system) with a resistivity of 18.3 MΩ·cm was used. The percentages mentioned throughout the paper are in molar fraction unless otherwise stated.

**Preparation of Vesicles.** Vesicles were prepared by extrusion as previously reported.[32] Briefly, phospholipid mixtures were obtained by mixing the appropriate volumes of phospholipid solutions in chloroform and allowed to dry in a stream of nitrogen, followed by desiccation under vacuum for 8 h to remove the residual organic solvent. The resulting phospholipid film was resuspended in Tris buffer overnight. The solution was then extruded 15 times through polycarbonate membranes (100 nm pore size) to produce uniform vesicles. The final concentration of the vesicles was 0.1 mg/mL. The average size of the resulting vesicles was in the range of 95−110 nm with a polydispersity index of 1.1 ± 0.05 by dynamic light scattering (Brookhaven 90plus/BI-MAS DLS, New York) at a scattering angle of 90°. The vesicles were freshly prepared for each experiment.

**Preparation of Polymer Cushion Layers.** The QCM sensor crystals (5 MHz) with a coating of gold were purchased from Q-SENSE (Gothenburg, Sweden). The crystal was cleaned by using piranha solution (concentrated $H_2SO_4$:30% $H_2O_2$ was 7:3 (v/v)), rinsed with large amounts of Milli-Q water, and blown dry with $N_2$. The cleaned crystal was initially exposed to an ethanol solution of MUA (2 mM) at room temperature for 24 h to form an SAM on Au surface. After rinsing with absolute ethanol and ultrapure water and drying in a nitrogen stream, the SAM surface was exposed to 0.2 M PDDA solution (concentration of monomer units) for 1 h at room temperature and then rinsed with Tris buffer and dried with $N_2$.

**Dissipative Quartz Crystal Microbalance.** Dissipative QCM measurements were performed with a QCM-Z500 system (KSV Instruments, Finland) equipped with a temperature control unit QCM-501.[40] The technique is based on the resonant oscillation of a piezoelectric quartz crystal disk at a frequency ($f$) and energy dissipation ($D$), which, respectively, characterize the mass and the viscoelastic property of the molecules adsorbed on the crystal surface. In vacuum or air, if the layer is rigid, evenly distributed, and much thinner than the crystal, $\Delta f$ is related to $\Delta m$ by the Sauerbrey equation,[41] $\Delta f = -n\Delta m/C_f$, where $n = 1, 3, 5, ...$, is the overtone number and $C_f = 17.7$ ng·cm$^2$·Hz$^{-1}$ at $f = 5$ MHz is the mass-sensitivity constant. The dissipation factor is defined by $\Delta D = E_d/2\pi E_s$,[42,43] where $E_d$ and $E_s$ are, respectively, the energies dissipated and stored during one cycle of oscillation. If not stated otherwise, dissipations and changes in normalized frequency of the third overtone ($n = 3$, i.e., 15 MHz) will be presented.

For a given experiment, the crystal covered with PDDA was initially exposed to Tris buffer and rinsed several times until the baseline was stable. Then, the buffer was replaced by a vesicle solution and the subsequent deposition of vesicles was monitored in time. All of the dissipative QCM measurements were carried out at 25 ± 0.1 °C.

**Atomic Force Microscopy.** AFM measurements were performed using a SEIKO SPA 300HV (Seiko Instruments Inc., Japan) scanning probe microscope equipped with an FS-150 V scanner (150 $\mu$m). Images were acquired under tapping mode at a scanning rate no greater than 0.5 Hz. The tapping mode was set at a resonant frequency of ∼20 kHz with low amplitude (0.3−0.4 V). Commercial silicon nitride cantilevers with a nominal force constant of 0.06 N/m (Veeco) were used. The fluid cell used for the AFM imaging was rinsed gently with buffer solution before scanning. All of the height images were flattened using second-order parameters unless otherwise stated.

A clean silicon wafer was used for the sputtering of a 5 nm thick adhesion layer of titanium and tungsten alloy followed by a 100 nm thick layer of gold. This gold-coated wafer was cut into slides of 15 × 15 mm. The formation of SAM on the slide and the subsequent adsorption of PDDA were similar to those on the QCM sensor crystals. The polymer-coated slide was affixed to a Teflon cell. Buffer solution was added and incubated for 1 h. The freshly prepared vesicle solution was

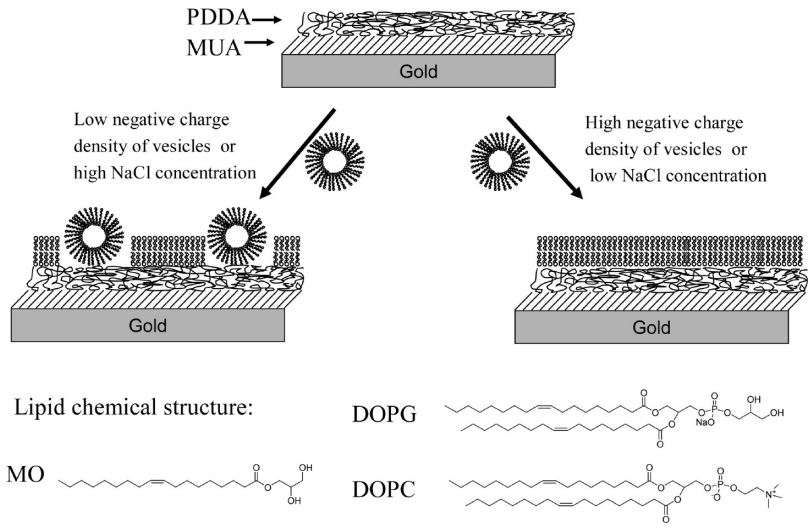


**Figure 1.** Schematic showing the formation of a phospholipid vesicle/bilayer mixture and complete coverage of a phospholipid bilayer supported by the PDDA/MUA layer on gold under different conditions. Chemical structures of DOPG, DOPC, and MO are also depicted.

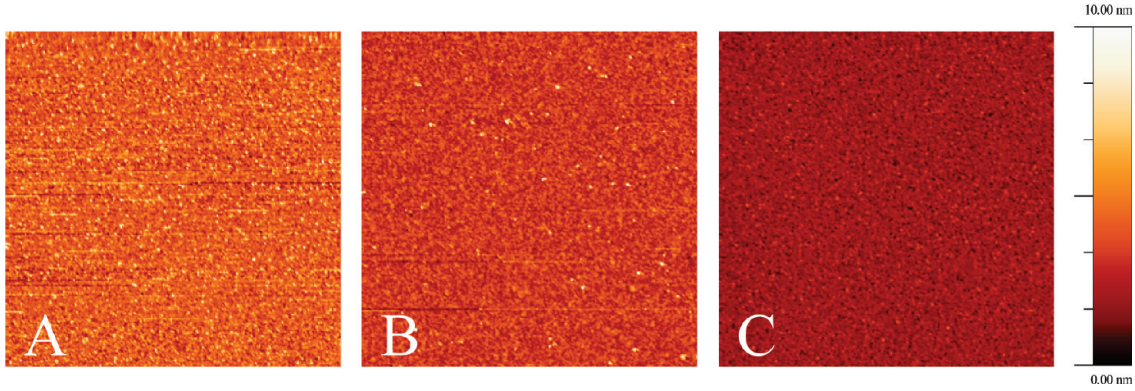


**Figure 2.** AFM surface morphology of the Au film (A), self-assembled monolayer of MUA on the gold film (B), and PDDA layer adsorbed on the MUA/Au surface (C). Image size: 4 × 4 $\mu$m.

then introduced into the cell in place of the buffer solution. The vesicle deposition lasted for 2 h before the cell was gently rinsed with excess amount of Tris buffer solution. The sample was imaged by AFM after being equilibrated for 30 min. All of the AFM measurements were conducted at room temperature.

## Results and Discussion

**Formation of PDDA Layers.** To construct polymer-supported planar lipid bilayers, we selected MUA to self-assemble a close-packed and ordered monolayer on a gold surface, as reported previously.[9] The p$K_a$ of the MUA molecule is 5.7 ± 0.2 in 0.10 M ionic strength solutions.[44] Thus the MUA layer at pH 8 bears a substantial amount of negative charges, which are needed for adsorbing positively charged PDDA chains by the electrostatic attraction. The positively charged PDDA is highly swollen in aqueous environments and thus can act as a deformable and mobile substrate for biomembranes to be made by depositing negatively charged vesicles. In order to investigate the vesicle−polyelectrolyte interaction and control the vesicle deposition and the subsequent transformation processes, we used binary lipid mixtures with tunable amounts of net negative charge, from negatively charged DOPG to amphiphilic natural lipid molecule MO and zwitterionic phospholipid DOPC. A schematic illustration of the PLBs assembly process and the lipid chemical structures are shown in Figure 1.

Figure 2 shows the formation of a PDDA polyelectrolyte film on a self-assembled monolayer of MUA on a gold-coated substrate. The gold film is uniform with a root-mean-square surface roughness (rms) of 1.31 nm over an area of 4 × 4 $\mu$m, as can be seen in Figure 2A. After the self-assembly of MUA on gold by chemisorption via the thiol group, the surface became more uniform with an rms of 0.90 nm (Figure 2B). While we could not measure the thickness of the MUA layer at this time, Zhang et al.[9] found that the MUA layer thickness is about 1.7 ± 0.2 nm under the same preparation. Shown in Figure 2C is a PDDA layer covered on the MUA surface with an rms of 0.58 nm, indicating a rather flat film, which is essential to the study of lipid bilayer formation by AFM.[16] Due to the fluid nature of the hydrated PDDA chains, the polyelectrolyte layer height could not be accurately measured by AFM. The thickness of the PDDA film in air was measured to be 2.1 ± 0.8 nm by ellipsometry (Model L116C, Gaertner Scientific Corp.), which is thicker than that observed by surface plasmon resonance (~1 nm).[8] It was previously shown that an increase of the ionic strength in the PDDA solution led to a larger amount of deposited polycations and thus to a thicker layer.[45,46] Therefore, the higher ionic strength of our buffer solution (including the extra 0.1 M NaCl) may account for this thickness disparity.

**Adsorption and Transformation of DOPG/MO Vesicles.** Figure 3 shows a series of AFM images of DOPG/MO vesicles with different molar ratios of DOPG/MO deposited on the PDDA film. The choice of MO lies in its tendency to assemble into nonlamellar phases, such as bicontinuous cubic phase and inverted hexagonal phase, which offers opportunities to tune

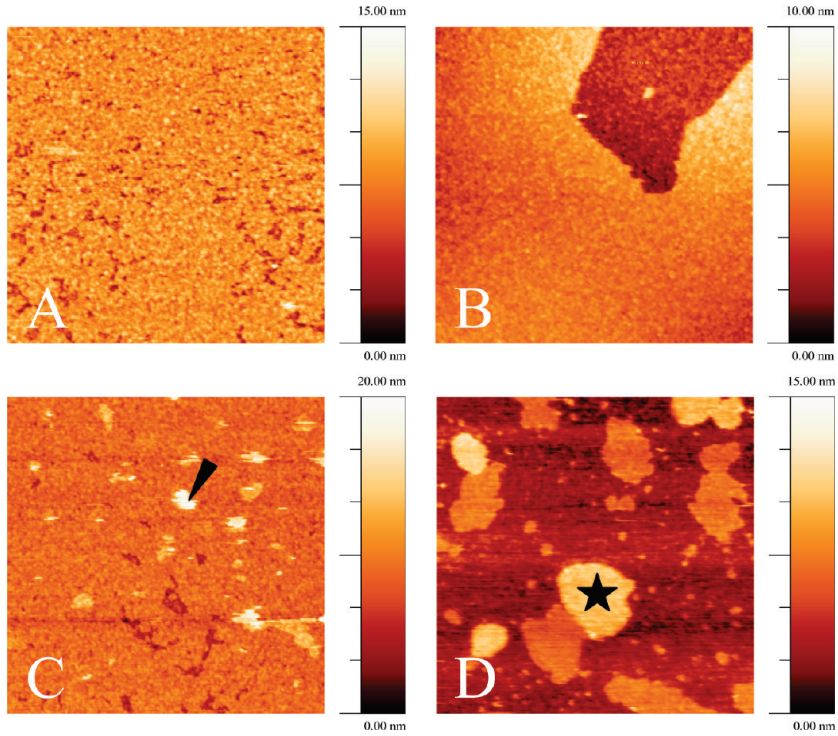


**Figure 3.** AFM images of the films obtained from the deposition of DOPG/MO vesicles on the PDDA/MUA/Au surface with different molar percentages of DOPG: (A) 100%, (B) 70%, (C) 50%, and (D) 30%. Image size: 4 × 4 $\mu$m.

membrane electrical/mechanical properties and study membrane lipid organizations and membrane dynamics, for example, membrane fusion.[32] For vesicles of pure DOPG and 70/30 of DOPG/MO, a new film is recognized and no adhered vesicle is found (Figure 3A,B). The film height is 4.8 ± 0.5 nm, which is about the thickness of a phospholipid bilayer, indicating the formation of a single phospholipid bilayer on the PDDA film. A careful examination of Figure 3A reveals many small holes or depressions in the bilayers due perhaps to the highest negative charge density on the pure DOPG used here, which could entail repulsion between the DOPG molecules, making the bilayers uneven. On the other hand, the deposition of vesicles containing 70% DOPG leads to the formation of a nice smooth bilayer (Figure 3B) possibly because the electrostatic repulsion between the DOPC molecules is decreased so that the bilayer can be close-packed. For 50/50 of DOPG/MO with an increasing content of MO (Figure 3C), a fairly good bilayer was still observable except for a few pinholes and adhered vesicles (see arrowhead). It is seen that the AFM image shown in Figure 3C contains tails along the scan direction, which were caused by a combination of weak AFM tip−sample interaction and low gains chosen for the image acquisition.[33] Finally, with a further increase of the MO molar fraction (DOPG/MO, 30/70, Figure 3D), only bilayer patches were observed and we also found some patches (see star in Figure 3D) with a height of 8.5 ± 0.7 nm, which corresponds to the thickness of a double bilayer. Because cubosomes tend to form when the molar fraction of MO becomes greater than 80% in the mixture,[32] we did not pursue further measurements beyond this composition. Taken together, these results clearly indicate that, with increasing DOPG content in the sample, the DOPG/MO vesicles are more predisposed to form PLBs.

The transformation process from isolated adsorbed DOPG/MO vesicles to a complete single bilayer on a PDDA surface was further investigated by using dissipative QCM. As shown in Figure 4 (also Figure S1 in the Supporting Information), after

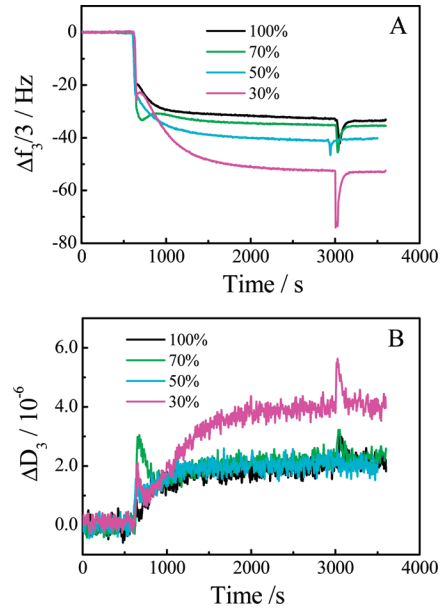


**Figure 4.** Real-time dissipative QCM responses, $\Delta f$ (A) and $\Delta D$ (B), during the deposition of DOPG/MO vesicles on the PDDA/MUA/Au surface with different molar percentages of DOPG.

the injection of a vesicle solution, the measured $\Delta f$ decreases and, simultaneously, $\Delta D$ increases monotonically until a stable value is reached within 40 min. No significant desorption was observed upon rinsing, indicating that the DOPG/MO system was deposited irreversibly and stably on the PDDA surface. By meticulously analyzing the final settled values of $\Delta f$ and $\Delta D$ in Figure 4 (also Figure S1 in the Supporting Information) as well as the AFM images in Figure 3, we find that the vesicle deposition can be classified into two groups. First, when the percentage of DOPG is greater than 60%, PLBs form (as confirmed by the AFM results described above) with $\Delta f = -(33-36)$ Hz and $\Delta D = (1.8-2.7) \times 10^{-6}$. These changes are

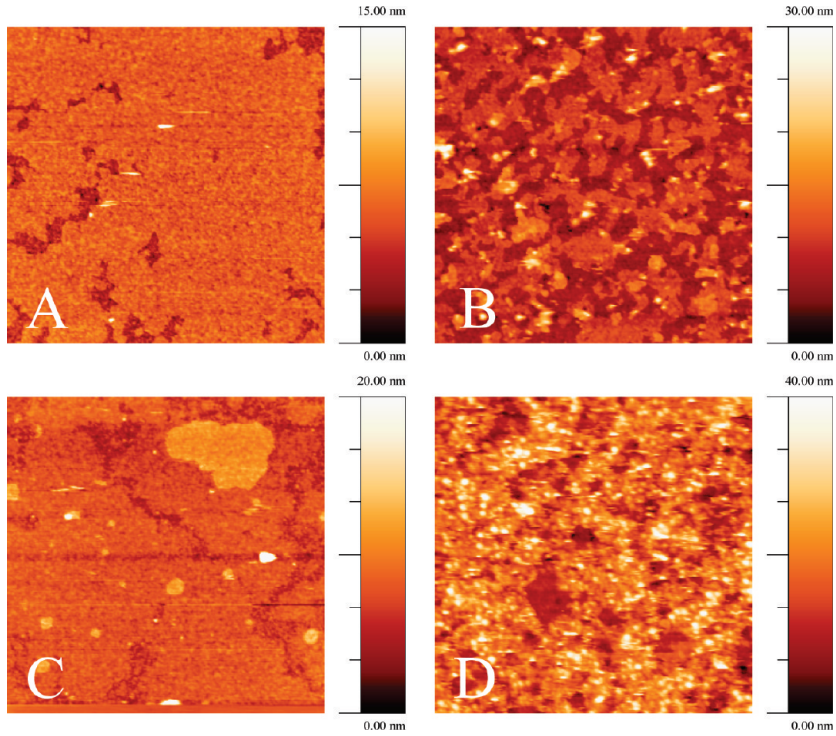


**Figure 5.** AFM images of the films obtained from the deposition of DOPG/DOPC vesicles on the PDDA/MUA/Au surface with different molar percentages of DOPG: (A) 80%, (B) 70%, (C) 50%, and (D) 30%. Image size: 4 × 4 $\mu$m.

relatively large compared to the characteristic values of $\Delta f$ ($\sim -25$ Hz) and $\Delta D$ ($<0.5 \times 10^{-6}$) for the formation of a solid-supported high-quality bilayer.[47,48] In particular, the dissipation shifts we observed are much larger than those for the formation of SLBs ($<0.5 \times 10^{-6}$), which would have been taken as evidence for adsorption of intact vesicles if a solid substrate were used. However, our substrate is a PDDA layer rather than a solid and the different softnesses of the substrates may result in very different dissipative QCM responses to the phospholipid bilayer formation. Dorvel et al.[49] reported that vesicles can be changed to a phospholipid bilayer on a tethered monolayer with values of $\Delta f$ and $\Delta D$ as high as $-115$ Hz and $45.0 \times 10^{-6}$, respectively. Although the phospholipid bilayer is rigid, the swollen polymer layer is known to be highly viscoelastic. Conceivably, the interaction of the viscoelastic polyelectrolyte chains with the phospholipid bilayer may render the energy dissipation to be much higher than commonly observed values in SLBs. As for the high $\Delta f$ observed in our experiment, we suspect that it is probably caused by abundant water trapped in the hydrophilic regions, say between the PDDA layer and the phospholipid bilayer. The second type of vesicle deposition is associated with lower molar percentage of DOPG in the phospholipid mixtures in the range of 30−50%, for which the measured $\Delta f$ is in the range between $-47$ and $-52$ Hz, and the corresponding $\Delta D$ is in the range between $2.7 \times 10^{-6}$ and $3.8 \times 10^{-6}$. These changes in frequency and dissipation are smaller than those expected for the sole deposition of intact vesicles but larger than those for the exclusive formation of a perfect bilayer.[33,34] These data thus suggest a partial adsorption of a small amount of intact vesicles or coexistence of bilayers and vesicles. The coexistence of bilayer patches and adsorbed vesicles is indeed observed in the AFM images shown in Figure 3C,D.

Electrostatic interactions can be invoked to explain the AFM and QCM-D results presented above. After the Au/MUA substrate was modified by cationic PDDA, negatively charged phospholipid molecules were adsorbed by the electrostatic attraction. The deposition of vesicles with different surface charge densities results in very dissimilar dissipative QCM responses and film structures. For pure DOPG vesicles with the highest negative charge density, the observed dissipative QCM response exhibits no minimum in frequency and maximum in dissipation (see Figure 4 and Figure S1 in the Supporting Information), implying that the vesicles, once adsorbed, cracked instantaneously to form a PLB without passing through a critical vesicle density.[34] This can be attributed to the strong vesicle−surface electrostatic attraction, which drives the fast rupture process. The addition of MO dilutes the negative charge density of DOPG/MO vesicles, leading to the weakening of the electrostatic attraction between vesicles and polymer layers. Consequently, the adsorption of vesicles becomes weaker and the rupture of vesicles becomes less probable. This is confirmed by the AFM images in Figure 3C,D. For the vesicles with 50% DOPG, PLBs could be formed although with a small amount of adsorbed vesicles (see Figure 3C). As the content of DOPG was further decreased to 30%, the weakened vesicle−surface attraction became insufficient to trigger the formation of PLBs. As a result, only some bilayer patches and double bilayer patches were observed (see Figure 3D). Correspondingly, the changes in frequency and dissipation were increased as can be seen in Figure 4 (also Figure S1 in the Supporting Information). In a word, it is clear that the electrostatic attraction between the polymer surface and the vesicle played a central role here in the formation of the PLBs.

**Adsorption and Transformation of DOPG/DOPC Vesicles.** To further confirm the effect of the electrostatic interaction on the PLB formation, we substitute DOPC for MO and study the deposition of the DOPG/DOPC vesicles onto the PDDA/MUA/Au surface. While MO is an amphiphilic neutral lipid molecule, DOPC is a zwitterionic phospholipid without carrying a net charge as a whole. Their molecular structures are shown in Figure 1. We first discuss the AFM results shown in Figure

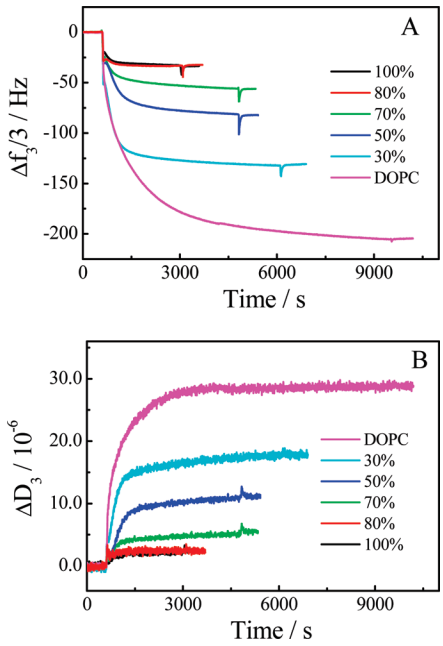


**Figure 6.** Real-time dissipative QCM responses, $\Delta f$ (A) and $\Delta D$ (B), during the deposition of DOPG/DOPC vesicles on the PDDA/MUA/Au surface with different molar percentages of DOPG.

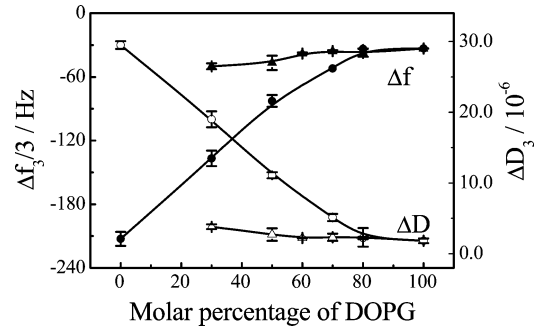


**Figure 7.** Measured $\Delta f$ and $\Delta D$ as a function of the molar percentage of DOPG for DOPG/MO (triangles) and DOPG/DOPC (circles) vesicle deposition on PDDA/MUA/Au surface. Each data point represents an average of at least three measurements. The error bars represent the standard deviations of the data.

5. For the DOPG/DOPC vesicles with a high percentage of DOPG (= 80%), the strong electrostatic attraction between the polymer film and the phospholipid headgroups appears to cause facile ruptures of the vesicle, as shown in Figure 5A. Consequently, a similar flat PLB was developed with a thickness of 4.8 ± 0.4 nm as in the case for the DOPG/MO vesicle system. For 70/30 of DOPG/DOPC, there are numerous bilayer patches together with some oblate vesicles, which have not completely ripped apart yet (Figure 5B). The corresponding $-\Delta f$ and $\Delta D$ (Figure 6) are 56 Hz and 5.5 × $10^{-6}$, respectively, a fact which is consistent with the existence of bilayer patches and oblate vesicles on the polymer film. For the vesicles with 50% DOPG (Figures 5C), although a bilayer can be clearly recognized, many patches are found above the bilayer with a thickness of 4.6 ± 0.2 nm. In other words, the patches are actually four layers. It appears that factors other than electrostatic interaction also need be considered here to account for the multibilayer formation. Finally, for vesicles with even lower net negative charge (DOPG/DOPC = 30/70), save for some bilayer patches, a stable vesicular layer with a highest attainable coverage is obtained (see Figure 5D). This effect is attributed to a combined weakening of the vesicle−support interaction and intervesicle repulsion.

Shown in Figure 6 are the dissipative QCM results for the DOPG/DOPC system. In general, the phospholipid mixtures with different compositions of DOPG and DOPC followed an adsorption kinetics similar to that of the DOPG/MO vesicles, i.e., having an initial rapid change in $\Delta f$ and $\Delta D$ followed by a gradual settling to an almost flat equilibrium level. For systems with a molar percentage of DOPG ≥80%, in which the formation of PLBs is confirmed by AFM imaging, the absence of a minimum in $\Delta f$ and a small value of $\Delta D$ suggest that the vesicles break up only after a short interaction time with the surface. In other words, no critical density of vesicles was observed for the bilayer formation. From Figure 6, we also find that the measured $-\Delta f$ and $\Delta D$ increase with decreasing molar percentage of DOPG, suggesting that the interaction between the vesicle and polymer support is becoming less attractive due to the reduced negative charge density of the vesicles. Finally, for pure DOPC vesicles, there was a large decrease in resonance frequency accompanied by an increase in dissipation factor shortly after the injection of the vesicles, which is a strong signature of the adhesion of intact vesicles to the PDDA layer. It is worth mentioning that a similar kinetics of vesicle deposition on PDDA has been reported by Stroeve et al. (refs 8−10) using the surface plasmon resonance technique. It was found that, for the deposition of a pure anionic lipid 1-stearoyl-2-oleoylphosphatidylserine (SOPC) and lipid mixtures of SOPC as a major component and 1-palmitoyl-2-oleoylphosphatidylcholine (POPC), the reflectivity profile echoed a rapid growth period followed by a slower approach to the flat equilibrium state within 1 h.. For pure POPC vesicles, however, the reflectivity kept increasing even 10 h after the injection of the vesicle solution. All of these results confirm that a high content of the negative charge bearing DOPG in the phospholipid mixtures can produce a strong attractive interaction between the surface and the vesicle, leading to a rapid rupture of the vesicles.

Although the vesicles of DOPG/MO and DOPG/DOPC display similar deposition kinetics, there is clearly a large difference in the magnitude of the response parameters extracted from the dissipative QCM data. The results are shown in Figure 7. The standard deviations were obtained by repeating each experiment at least three times. When the molar percentage of DOPG is above 80, the changes in frequency and dissipation are similar for both systems, pointing to similar properties of the PLBs formed. With decreasing molar fraction of DOPG in the vesicles, the measured values of $-\Delta f$ and $\Delta D$ for DOPG/MO become smaller than those for DOPG/DOPC, suggesting that the DOPG/MO vesicles form bilayers more readily, whereas the DOPG/DOPC phospholipids are more prone to adsorb on the PDDA surface as intact vesicles. This inference can be appreciated from Figures 3 and 5. Although the zwitterionic DOPC molecule does not carry a net charge as a whole, its positive charge is closer to the surface of the DOPG/DOPC vesicle than the negative one, so that the dipole of the zwitterions in the headgroups in effect decreases the net charge density of the vesicle.[38] This will have a weakening effect on the attraction between the substrate and vesicle. To come to the point, the PDDA surface has a stronger electrostatic attraction to the DOPG/MO vesicles compared with the DOPG/DOPC vesicles at the same mole fraction of DOPG, giving rise to a more facile formation of bilayers.

**Effect of NaCl Concentration on PLB Formation.** To further confirm the central role played by the electrostatic interaction in PLB formation, we studied the effect of salt concentration on the adsorption and rupture of the DOPG/DOPC

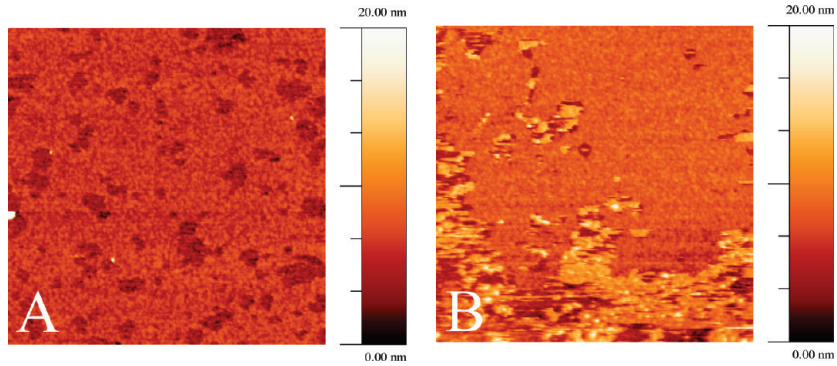


**Figure 8.** AFM images of the films obtained from the deposition of DOPG/DOPC (molar ratio 50/50) vesicles on the PDDA/MUA/Au surface at different concentrations of NaCl: (A, left) 0 and (B, right) 500 mM. Image size: 4 × 4 $\mu$m.

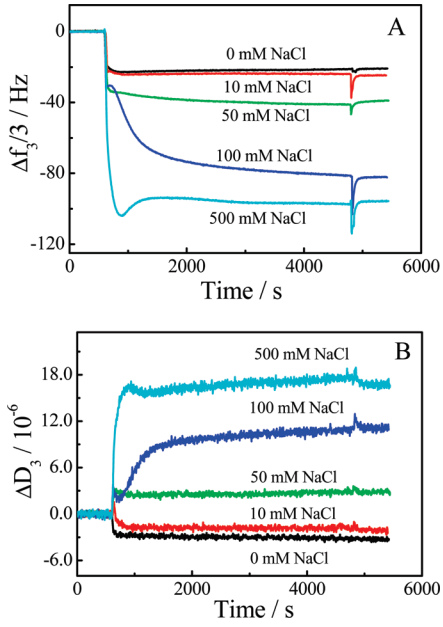


**Figure 9.** Real-time dissipative QCM responses, $\Delta f$ (A) and $\Delta D$ (B), during the deposition of DOPG/DOPC (molar ratio 50/50) vesicles on the PDDA/MUA/Au surface at different concentrations of NaCl.

(50/50) vesicles using the techniques of AFM and dissipative QCM. We prepared 0.1 mg/mL vesicle solutions in Tris solutions with 500, 100, 50, 10, and 0 mM NaCl, respectively. Presented in Figure 8A and 8B are the AFM images obtained for the DOPG/DOPC vesicles adsorbed on a PDDA layer with 0 and 500 mM NaCl, respectively. As clearly shown in Figure 8A, in the absence of NaCl, the DOPG/DOPC vesicles form a nice flat bilayer on PDDA. However, with a 500 mM NaCl solution (see Figure 8B), about 30% areas on PDDA are covered by intact vesicles in addition to the PLBs. The corresponding dissipative QCM data in Figure 9 show large changes in dissipation and frequency for the 50 mM and, to a larger extent, 500 mM NaCl solutions, signifying a soft structure formed on the polymer surface. However, for the 10 and 0 mM NaCl solutions, the measured values of $\Delta f \sim -21$ and $-25$ Hz, respectively, are the characteristic values for PLB formation. It is noted that the dissipation after the bilayer formation is somewhat lower than that of the PDDA layer prior to the bilayer adhesion. We speculate that, in low ion concentrations, the unscreened charges of PDDA chains repel each other to maximize interchain distances, leading to a relatively high viscoelasticity for the polyelectrolyte film. Consequently, after the relatively rigid bilayer covers the PDDA surface, the viscoelasticity of the whole film is reduced, namely there is a decline of $\Delta D$.

By combining the AFM images with the QCM-D results presented above, we conclude that the amount of adsorbed vesicles increases with the NaCl concentration. To be precise, in zero or low ionic strength solutions, the vesicles tend to rupture and form a bilayer on PDDA. By all accounts, the addition of ions in a solution will screen out the electrostatic force and thus weaken the vesicle−substrate attraction and vesicle−vesicle repulsion. Boudard et al.[37] found that, in the absence of salt, strong vesicle−solid surface interactions took place and favored a fast vesicle rupture process. In a similar vein, Seantier and Kasemo[38,48] suggested that an increasing ion concentration has a stabilizing effect on vesicles. However, there are also conflicting reports indicating the destabilization of vesicles in high ionic strength solutions.[50] Our results reinforce the notion that the electrostatic attraction is mostly responsible for inducing the vesicle rupture and PLB formation. In our system, the PDDA molecule bears a high positive charge density, so that the electrostatic shielding in a high ionic strength solution diminishes the repulsion between the polymer chains,[16] which will weaken the vesicle−surface attraction. In addition, for the negatively charged vesicles, the charge shielding effect results in a smaller repulsion between the vesicles. Both effects will in turn stabilize the vesicles and allow them to adsorb on the PDDA surface.

**Pathways of Vesicle Deposition on PDDA Substrate.** Overall, there are four different pathways for the vesicle deposition on a solid support, which can be followed by dissipative QCM:[39] (i) no vesicle adsorption, (ii) intact vesicle adsorption, (iii) bilayer formation through a critical vesicle coverage, and (iv) bilayer formation through direct rupture of individual vesicles. Because the former two pathways have no bilayer formation, we focus on the latter two pathways (called pathway 1 and pathway 2, respectively, hereafter), which lead to bilayer formation via two different processes. The two processes are mainly governed by three types of interactions:[33,48] supported-surface−vesicle interaction, intervesicle interaction, and intravesicle molecular interaction. In the case of pathway 1, the relatively low adhesion strength between the substrate and phospholipids stabilizes the vesicles deposited on the surface. As more vesicles are adsorbed, the vesicle−vesicle interaction comes into play so that when a critical surface coverage is reached, the vesicle rupture and bilayer formation will occur. In this scenario, the QCM frequency decreases first due to the continuous vesicle adsorption and then increases because of vesicle rupture beyond a critical vesicle density. The dissipation will experience similar changes but in opposite directions. For pathway 2, the strong substrate−vesicle attraction coerces the vesicles to break only after a short interaction time with the substrate. In this case, the frequency (dissipation) will

decrease (increase) monotonously. Several studies have pointed out the influences of the charges of the substrate and phospholipids as well as the ionic strength of solution on the deposition of vesicles on solid supports.[33,48,50−53] Richter et al.[33,39,54] reported that the vesicle charge is a determining parameter for the vesicle decomposition pathway. It is commonly believed that the bilayer-formation process will be strongly affected by electrostatic interactions. Accordingly, for a given surface, the pathway of bilayer formation can be optimized by adjusting the charge density of the vesicle surface, pH, or ionic strength of the solution. However, by changing these parameters, we failed to find a critical vesicle coverage by dissipative QCM for all of the samples we have studied, although bilayers, patches, and intact vesicles are observed by AFM. In other words, the pathway of PLB formation in our case is not affected by altering the vesicle charge and ionic strength of the solution.

It should be pointed out that the PDDA polymer support is different from the solid substrate in that it is made of a hydrophilic soft material. For phospholipid vesicles with a high mole fraction of DOPG, its surface carries many negative charges. This gives rise to a strong vesicle−surface attraction, which as a result enlarges the contact area and leads to the vesicle destabilization and thus a fast rupture of the vesicles. It follows that there will be no critical coverage density for vesicles on the PDDA surface, which is consistent with our observation. As MO or DOPC is added into the phospholipid mixtures, the vesicles tend to be stabilized on the PDDA layer due to charge dilution. However, even when a large number of vesicles were adsorbed, we did not observe any vesicle rupture process. This in effect excludes pathway 1 for our vesicle deposition process. We propose that, due to water swelling, highly hydrated PDDA chains extend into the aqueous solution and probably form a brushlike configuration on its surface. These polymer chains can trap some vesicles, or even form polymer−vesicle aggregates in the interfacial layer.[13] In other words, the soft and fluctuating substrate can weaken the vesicle−vesicle interaction and prohibit intervesicle fusion. Under these conditions, intact vesicles can be deposited on the PDDA layer even at a high surface coverage.

## Conclusion

We have used the techniques of AFM and dissipative QCM to identify and characterize the deposition process of phospholipid vesicles on a PDDA film. Vesicles of variable compositions can be deposited and form PLBs by increasing the negative charge density on the vesicles or decreasing the ionic strength of the solution. Our work manifests that the electrostatic attraction between the substrate and vesicle is the driving force for the rupture of vesicles and the PLB formation. The most important pathway responsible for the bilayer formation is found to be a fast adsorption−rupture process of the vesicles, which is always operative under our experimental conditions irrespective of the charge density on the vesicles and the ionic strength of the solutions. The soft polymer support is shown to be proactive in triggering and influencing the PLB-formation process. Our results suggest that the molecular-level interaction between the phospholipids and polymer chains can weaken the vesicle−vesicle interaction and prevent the vesicles from fusion. Such a polymer cushion can act as an ideal lubricating layer between the bilayer and the substrate and allow for incorporating biomolecules such as transmembrane proteins to the supported bilayer without the risk of direct contact with the bare substrate surface.

**Acknowledgment.** This work was supported by the Hong Kong Research Grants Council (RGC) General Research Funds (GRF) No. HKUST 604608. We thank the HKUST University Research Equipment Fund for support of AFM upgrades.

**Supporting Information Available:** Real-time dissipative QCM responses for the deposition of DOPG/MO vesicles on the PDDA/MUA/Au surface. This information is available free of charge via the Internet at http://pubs.acs.org.

## References and Notes

(1) Sackmann, E. *Science* **1996**, *271*, 43–48.
(2) Castellana, E. T.; Cremer, P. S. *Surf. Sci. Rep.* **2006**, *61*, 429–444.
(3) Tanaka, M.; Sackmann, E. *Nature* **2005**, *437*, 656–663.
(4) Tamm, L. K.; Mcconnell, H. M. *Biophys. J.* **1985**, *47*, 105–113.
(5) Groves, J. T.; Mahal, L. K.; Bertozzi, C. R. *Langmuir* **2001**, *17*, 5129–5133.
(6) Li, E.; Hristova, K. *Langmuir* **2004**, *20*, 9053–9060.
(7) Tanaka, M.; Sackmann, E. *Phys. Status Solidi A* **2006**, *203*, 3452–3462.
(8) Zhang, L. Q.; Longo, M. L.; Stroeve, P. *Langmuir* **2000**, *16*, 5093–5099.
(9) Zhang, L.; Vidu, R.; Waring, A. J.; Lehrer, R. I.; Longo, M. L.; Stroeve, P. *Langmuir* **2002**, *18*, 1318–1331.
(10) Ma, C.; Srinivasan, M. P.; Waring, A. J.; Lehrer, R. I.; Longo, M. L.; Stroeve, P. *Colloids Surf., B* **2003**, *28*, 319–329.
(11) Luo, G. X.; Wang, H. P.; Jin, J. *Langmuir* **2001**, *17*, 2167–2171.
(12) Majewski, J.; Wong, J. Y.; Park, C. K.; Seitz, M.; Israelachvili, J. N.; Smith, G. S. *Biophys. J.* **1998**, *75*, 2363–2367.
(13) Wong, J. Y.; Majewski, J.; Seitz, M.; Park, C. K.; Israelachvili, J. N.; Smith, G. S. *Biophys. J.* **1999**, *77*, 1445–1457.
(14) Wong, J. Y.; Park, C. K.; Seitz, M.; Israelachvili, J. *Biophys. J.* **1999**, *77*, 1458–1468.
(15) Kugler, R.; Knoll, W. *Bioelectrochemistry* **2002**, *56*, 175–178.
(16) Luo, G. B.; Liu, T. T.; Zhao, X. S.; Huang, Y. Y.; Huang, C. H.; Cao, W. X. *Langmuir* **2001**, *17*, 4074–4080.
(17) Munro, J. C.; Frank, C. W. *Langmuir* **2004**, *20*, 10567–10575.
(18) Munro, J. C.; Frank, C. W. *Langmuir* **2004**, *20*, 3339–3349.
(19) Hwang, L. Y.; Gotz, H.; Hawker, C. J.; Frank, C. W. *Colloids Surf., B* **2007**, *54*, 127–135.
(20) Hwang, L. Y.; Gotz, H.; Knoll, W.; Hawker, C. J.; Frank, C. W. *Langmuir* **2008**, *24*, 14088–14098.
(21) Deverall, M. A.; Garg, S.; Ludtke, K.; Jordan, R.; Ruhe, J.; Naumann, C. A. *Soft Matter* **2008**, *4*, 1899–1908.
(22) Beyer, D.; Elender, G.; Knoll, W.; Kuhner, M.; Maus, S.; Ringsdorf, H.; Sackmann, E. *Angew. Chem., Int. Ed.* **1996**, *35*, 1682–1685.
(23) Diaz, A. J.; Albertorio, F.; Daniel, S.; Cremer, P. S. *Langmuir* **2008**, *24*, 6820–6826.
(24) Wagner, M. L.; Tamm, L. K. *Biophys. J.* **2000**, *79*, 1400–1414.
(25) Kiessling, V.; Tamm, L. K. *Biophys. J.* **2003**, *84*, 408–418.
(26) Merzlyakov, M.; Li, E.; Gitsov, I.; Hristova, K. *Langmuir* **2006**, *22*, 10145–10151.
(27) Baumgart, T.; Offenhausser, A. *Langmuir* **2003**, *19*, 1730–1737.
(28) Goennenwein, S.; Tanaka, M.; Hu, B.; Moroder, L.; Sackmann, E. *Biophys. J.* **2003**, *85*, 646–655.
(29) Hillebrandt, H.; Wiegand, G.; Tanaka, M.; Sackmann, E. *Langmuir* **1999**, *15*, 8451–8459.
(30) Berquand, A.; Mazeran, P. E.; Pantigny, J.; Proux-Delrouyre, V.; Laval, J. M.; Bourdillon, C. *Langmuir* **2003**, *19*, 1700–1707.
(31) Shen, W. W.; Boxer, S. G.; Knoll, W.; Frank, C. W. *Biomacromolecules* **2001**, *2*, 70–79.
(32) Wang, Z. N.; Yang, S. H. *Langmuir* **2008**, *24*, 11616–11624.
(33) Richter, R.; Mukhopadhyay, A.; Brisson, A. *Biophys. J.* **2003**, *85*, 3035–3047.
(34) Reimhult, E.; Hook, F.; Kasemo, B. *Langmuir* **2003**, *19*, 1681–1691.
(35) Jass, J.; Tjarnhage, T.; Puu, G. *Biophys. J.* **2000**, *79*, 3153–3163.
(36) Seantier, B.; Breffa, C.; Felix, O.; Decher, G. *Nano Lett.* **2004**, *4*, 5–10.
(37) Boudard, S.; Seantier, B.; Breffa, C.; Decher, G.; Felix, O. *Thin Solid Films* **2006**, *495*, 246–251.
(38) Seantier, B.; Kasemo, B. *Langmuir* **2009**, *25*, 5767–5772.
(39) Richter, R. P.; Berat, R.; Brisson, A. R. *Langmuir* **2006**, *22*, 3497–3505.
(40) Viitala, T.; Hautala, J. T.; Vuorinen, J.; Wiedmer, S. K. *Langmuir* **2007**, *23*, 609–618.
(41) Sauerbrey, G. *Z. Phys.* **1959**, *155*, 206–222.
(42) Rodahl, M.; Hook, F.; Krozer, A.; Brzezinski, P.; Kasemo, B. *Rev. Sci. Instrum.* **1995**, *66*, 3924–3930.
(43) Voinova, M. V.; Rodahl, M.; Jonson, M.; Kasemo, B. *Phys. Scr.* **1999**, *59*, 391–396.

(44) Smalley, J. F.; Chalfant, K.; Feldberg, S. W.; Nahir, T. M.; Bowden, E. F. *J. Phys. Chem. B* **1999**, *103*, 1676–1685.
(45) Ladam, G.; Schaad, P.; Voegel, J. C.; Schaaf, P.; Decher, G.; Cuisinier, F. *Langmuir* **2000**, *16*, 1249–1255.
(46) Kleinfeld, E. R.; Ferguson, G. S. *Science* **1994**, *265*, 370–373.
(47) Keller, C. A.; Kasemo, B. *Biophys. J.* **1998**, *75*, 1397–1402.
(48) Seantier, B.; Breffa, C.; Felix, O.; Decher, G. *J. Phys. Chem. B* **2005**, *109*, 21755–21765.
(49) Dorvel, B. R.; Keizer, H. M.; Fine, D.; Vuorinen, J.; Dodabalapur, A.; Duran, R. S. *Langmuir* **2007**, *23*, 7344–7355.
(50) Cremer, P. S.; Boxer, S. G. *J. Phys. Chem. B* **1999**, *103*, 2554–2559.
(51) Hennesthal, C.; Steinem, C. *J. Am. Chem. Soc.* **2000**, *122*, 8085–8086.
(52) Radler, J.; Strey, H.; Sackmann, E. *Langmuir* **1995**, *11*, 4539–4548.
(53) Dimitrievski, K.; Kasemo, B. *Langmuir* **2008**, *24*, 4077–4091.
(54) Richter, R. P.; Brisson, A. R. *Biophys. J.* **2005**, *88*, 3422–3433.

JP9068224